The Journal of Chemical Physics ARTICLE scitation.org/journal/jcp

Microdroplets can act as electrochemical cells

Cite as: J. Chem. Phys. 156, 054705 (2022); doi: 10.1063/5.0078281
Submitted: 11 November 2021 • Accepted: 10 January 2022 •
Published Online: 2 February 2022

View Online Export Citation CrossMark

Christian F. Chamberlayne and Richard N. Zare[a)]

AFFILIATIONS

Department of Chemistry, Stanford University, Stanford, California 94305, USA

[a)]Author to whom correspondence should be addressed: zare@stanford.edu

ABSTRACT

A water microdroplet in air or oil typically possesses an electric double layer (EDL) from the preferential adsorption of surface-bound ions at the periphery. We present the calculations of the ion gradients within a microdroplet at equilibrium, including systems containing buffers and water autoionization. These ion gradients are used to calculate the potential energy stored within the microdroplet. We consider how this stored potential energy can be utilized to drive chemical reactions, much like an electrochemical cell. Effective voltages as high as 111 mV are found for microdroplets having a low surface charge density (0.01 ions per nm^2). Two sources of potential energy are investigated: (1) the electrostatic energy of the EDL of the microdroplet and (2) shifts in other chemical equilibria coupled to the main reaction through the EDL. A particularly important example of the latter is water autoionization, wherein the reaction of interest causes a flattening of the $[H^+]$ gradient within the EDL, resulting in a net recombination of H^+ and OH^- throughout the microdroplet. Numerical calculations are performed using a continuum model consisting of a balance between the electromigration and diffusion of ions throughout the microdroplet. Our treatment accounts for the autoionization of water and any chemical equilibrium of buffers present. The results are presented for uncharged water microdroplets with low amounts of salts and simple buffers in them. However, the calculational method presented here can be applied to microdroplets of any net charge, composed of any solvent, containing ions of any valence, and containing complex mixtures of chemical equilibria.

Published under an exclusive license by AIP Publishing. https://doi.org/10.1063/5.0078281

INTRODUCTION

Microdroplets are emerging as an interesting medium for chemistry. They exhibit a surprisingly complex structure compared to the typical expectation of them as tiny reaction beakers. Some species localize to the atomic interface of the microdroplets, and these species exhibit a variety of interesting chemistry caused by their two-dimensional confinement, surface electric fields, and partial solvation. Much attention has been paid to this area in microdroplets.[1–4] Less attention has been given to effects on chemical reactions from the macroscopic properties of the microdroplet. One notable paper on how the reactant concentration and compartment size together lead to accelerated reaction rates under micro-confinement is the work by Wilson and co-workers,[5] wherein they show how changes in the reaction rates at the surface can affect the interior concentration of the microdroplet in a size-dependent manner.

The localization of species (such as surfactants) to the atomic interface includes charged ions. This typically results in a net surface charge density of a microdroplet. The net surface charge density is often incorrectly conflated with the net total charge on the microdroplet. The surface-bound ions can have counterions that are dissolved into the interior of the microdroplet. Thus, a microdroplet can have a large net surface charge density while being completely net neutral. This situation is pictured in Fig. 1 with the surface-bound ions arbitrarily chosen as negative. For the cases of aerosols without a deliberately added surfactant, the origin of the surface charge in water droplets has been a topic of contention as to whether it arises from the preferential adsorption of OH^- or from some anionic surfactant.[6,7] However, Ganachaud and co-workers[8] presented strong evidence that the negative surface charge in aerosols originates from small amounts of dissolved carbon dioxide, producing the bicarbonate anion (HCO_3^-) at the periphery.

This separation of charges into surface-bound and dissolved leads to a radial electric field originating inside the droplet and terminating on the ions at its surface. We have discussed previously the effects that this electric field can have on reactions taking place inside the microdroplet.[9] Electric fields are known to have effects on chemical reactions in a variety of different environments.[4,10–17] While not the main focus of this paper, the effect of this internal electric field in the microdroplet on chemical reactions should not be overlooked.

Published under an exclusive license by AIP Publishing

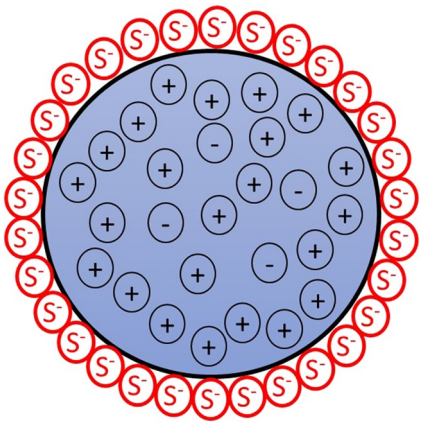

FIG. 1. Illustration of the microdroplet with charged surface-bound ions with dissolved counterions.

Expanding on our previous work,[9] we first concern ourselves with the equilibrium ion distributions in a microdroplet that also contains chemical equilibria, such as water autoionization and buffer solutions. To reach equilibrium in a microdroplet, there is a shift in the chemical equilibrium from the bulk solution amount, typically toward the side of the equilibrium that creates more ions. This shift is a direct result of the ion gradients in the electric double layer (EDL) of the microdroplet. Importantly, it can result in a vastly different chemical environment inside a microdroplet as compared to a bulk solution.

We are interested in the potential energy stored in the macroscopic ion configuration of the microdroplet. There are two sources we focus on in this paper. First, the shift in chemical equilibrium away from the equilibrium of the bulk solution stores chemical potential energy in the microdroplet. Second, the EDL itself stores electrostatic potential energy from the separation of charges within it. Using the model in this paper to find the ion gradients in the microdroplet, we can then assign numerical values to the stored potential energy.

Finally, we are interested in how the potential energy in the microdroplet might be applied to a chemical reaction taking place within it. We hypothesize that the aforementioned potential energy of a microdroplet can change as a result of a chemical reaction, particularly for cases where the chemical reaction lowers the surface charge density of the microdroplet by reacting with the surface-bound ions. This hypothesized mechanism may help explain the source of energy for unusual redox activity previously observed in microdroplets.[18–23]

We consider a slow chemical reaction taking place in an adiabatic manner in the microdroplet. By adiabaticity, we mean that the chemical reaction of interest happens on a significantly slower timescale than the stabilization of the EDL in the microdroplet. This is a reasonable assumption as ion motion in an EDL, water autoionization, and the protonation reaction in buffers are all fast processes. With this adiabatic assumption, we can use the equilibrium ion distribution in the microdroplet as a pseudo-steady-state from which to calculate the macroscopic potential energy change in the microdroplet at different points along the progression of the reaction of interest. A change in the potential energy of the system acts as an additional driving force on the reaction.

Comparison to an electrochemical cell makes for a good qualitative description of the mechanism we propose. The microdroplet has two separated regions of charge: a surface charge arising from ionic surface-bound species (i.e., surfactants) and an interior volume charge arising from their dissolved counterions, as depicted in Fig. 1. Chemical reactions that move charge from one region to the other gain an additional driving force. This behavior is quite similar to an electrochemical cell where reactions that transfer charge from one electrode to the other are driven by the applied voltage.

Ion distributions in microdroplets

In a microdroplet, the flux of ions is governed by two competing effects, namely, diffusion and electromigration. The electric field causing the electromigration is a direct result of the charge separation in the microdroplet. At equilibrium, these two fluxes are equal and oppositely directed, that is, they balance one another as follows:

$$-z_i c_i \nabla \varphi = V_T \nabla c_i. \tag{1}$$

Here, z_i is the ion charge (unitless but signed), c_i is the local concentration of the ith species (mole m^{-3}), φ is the electric potential (V), V_T is the thermal voltage (25.7 mV at 25 °C), and D_i is the diffusion coefficient (m^2 s^{-1}). The electric fields in the microdroplet are governed by the differential form of Gauss's law as follows:

$$\nabla \cdot (\varepsilon \nabla \varphi) = -\rho, \tag{2}$$

where ρ is the local charge density (mole m^{-3}) and ε is the dielectric constant (C V^{-1} m^{-1}). Substitution of Eq. (1) into Eq. (2) sets up a second-order differential equation in spherical coordinates. The boundary conditions for the differential equation can be determined by enforcing that there are a fixed number of each type of strong electrolyte ion within the microdroplet. In the section titled Calculations and our previous work, we described how to numerically calculate the resulting internal electric fields and ion gradients within microdroplets from these governing equations.[9] The resulting ion gradients in the microdroplet follow a Boltzmann distribution as derived in the section titled Calculations at the end of this manuscript. We have previously shown that for systems following a Boltzmann distribution of ions, chemical equilibrium is also achieved throughout the EDL.[24] This includes [H$^+$] gradients inside EDLs being stable despite the presence of a buffer.

Ion distributions in microdroplets of unbuffered salt water

For simplicity in considering the large parameter space of possible microdroplet chemical compositions, we first restrict our discussion to a water microdroplet having zero net charge and a negatively charged surfactant in which the only ions present in the microdroplet are uni-univalent (ion valence ±1 only) strong electrolytes and those from water autoionization. The full derivation is presented separately in the section titled Calculations at the end of this manuscript. The resulting governing equation is as follows:

Published under an exclusive license by AIP Publishing

$$\frac{1}{r^2}\frac{\partial}{\partial r}\left(r^2\frac{1}{[\mathrm{H}^+]}\frac{\partial[\mathrm{H}^+]}{\partial r}\right) = \frac{F}{V_T\,\varepsilon}\left\{(1+R_+)[\mathrm{H}^+] + (1+R_-)K_w/[H^+]\right\}, \tag{3}$$

where r is the radial distance from the microdroplet center, F is Faraday's constant, V_T is the thermal voltage (25.7 mV at 25 °C), ε is the dielectric constant of water, and K_w is the equilibrium constant for the autoionization of water. R_+ and R_- are unknown parameters in the differential equation and are determined based on the boundary conditions of the differential equation. They represent the ratio of the +1 charged strong electrolytes to H^+ ions and the ratio of the −1 charged strong electrolytes to OH^- ions, respectively.

There are four boundary conditions as it is a second-order differential equation with two unknown parameters (R_+ and R_-),

$$\nabla\left[H^+\right] = 0 \text{ at center of the droplet}, \tag{4}$$

$$\text{total surface charge} + \iiint_V \rho\, dV = 0, \tag{5}$$

$$\iiint_V c_+ dV = \text{moles of} + 1 \text{ ion in the droplet}\left(\text{excluding } \mathrm{H}^+\right), \tag{6}$$

and

$$\iiint_V c_- dV = \text{moles of} - 1 \text{ ion in the droplet}\left(\text{excluding } \mathrm{OH}^-\right), \tag{7}$$

where c_+ and c_- are the concentrations of the +1 and −1 valence strong electrolytes, respectively. The boundary condition given in Eq. (5) ensures that the droplet is net neutral. Adjusting this boundary condition allows for charged droplets to be evaluated. For a charged droplet, the boundary condition given by Eq. (5) is replaced with

$$\text{total surface charge} + \iiint_V \rho\, dV = \text{net droplet charge}. \tag{8}$$

A few notable conclusions from the derivation are worth mentioning. First, ions of the same valence will have a constant ratio between their concentrations throughout the microdroplet. Second, unlike in the case of strong electrolytes, the moles of H^+ ions and OH^- ions within the microdroplet can change from that of the droplet precursor solution to reach an equilibrium solution in the microdroplet that satisfies the equilibrium constant for the autoionization of water (K_w) at all locations. This means that the moles of H^+ ions and OH^- ions within the microdroplet are not useful as a boundary condition. Instead, the constraint of equilibrium constant for the autoionization of water (K_w) at all locations is enforced by the governing equation (3).

The governing equation, Eq. (3), is derived in the section titled Calculations and solved numerically using MATLAB®. Figure 2 shows the calculated ion distributions for two different microdroplets. Both are 5 μm diameter neutral aqueous microdroplets with a surface charge density of 0.01 ions per nm^2 at 25 °C. They differ in their internal ion average concentrations with the 100 nM negative strong electrolyte and 20.0 μM positive strong electrolyte for one microdroplet and 1 μM negative strong electrolyte and 20.9 μM positive strong electrolyte for the other. An example for Fig. 2(a) would be a 5 μm diameter aqueous microdroplet formed from a precursor solution of 19.9 μM sodium dodecyl sulfate (SDS) and 100 nM NaCl. We assume that the dodecyl sulfate ions from the SDS surfactant fully adsorb to the surface, thereby giving it a 0.01 ions per nm^2 surface charge density. An example for Fig. 2(b) would be a 5 μm diameter aqueous microdroplet formed from a precursor solution of 19.9 μM SDS and 1 μM NaCl. The microdroplet with a lower average concentration of ions shows a thicker EDL. This correlates nicely with the Gouy–Chapman model for a one-dimensional EDL, wherein lower ionic strength results in a larger Debye length.[25]

A particularly notable feature is the $[H^+]$ gradient inside the microdroplet. The H^+ ions are drawn toward the negatively charged microdroplet surface while being depleted from the interior of the microdroplet, resulting in an acidic outer region and a basic center in the microdroplet. This trend is reversed for the case of a positively charged surface-bound ion, giving a positive charge to the periphery of the microdroplet. The same trend for a $[H^+]$ gradient in microdroplets was calculated by Kwan and Consta[26] for highly charged microdroplets.

Because the activity differs from the concentration in the presence of an electric field, we specifically refer to $-\log_{10}[H^+]$ and $-\log_{10}[OH^-]$ for describing a microdroplet rather than pH and pOH, as the latter is defined by the activity of H^+ and OH^-. Figure 2 provides a good example of how the moles of H^+ and OH^- are not conserved. Both the $-\log_{10}(\text{average}[H^+])$ and $-\log_{10}(\text{average}[OH^-])$ of the microdroplet are 6.5 for the microdroplet shown in Fig. 2(a) and 6.6 in Fig. 2(b). The microdroplet contains acidic and basic regions such that the sum of the negative log of the two averages is not 14 as might have first been expected.

Both microdroplets in Fig. 2 have the same electric field strength (2.3×10^6 V m^{-1}) at the periphery of the microdroplet as this is a function of the droplet radius and surface charge density. They differ in how quickly the electric field dies off. We observe that as the ionic strength increases, which causes the EDL to thin, the electric field strength decreases on average throughout the microdroplet. As a result of the spherical geometry, about half the volume of a 5-μm diameter microdroplet is located within 500 nm of the periphery where the electric field strength is roughly between 10^5 and 10^6 V m^{-1} in our examples. Even with the low surface charge density of this example, the electric field strengths begin to approach the limit imposed by the dielectric strength of water of 6.5×10^7 to 7×10^7 V/m, above which bulk water ionizes.[27] The presence of the electric field in the EDL can affect chemical reaction rate constants via numerous mechanisms, including the alignment of the reactants, alteration of the solvent cage, and stabilization of transition state dipoles. We have discussed these effects on chemical reactions in microdroplets in more detail in our previous work.[9]

Ion distributions in buffered solutions

Buffered solutions add an extra layer of complexity to the ion distribution. The moles of species within the microdroplet change from the droplet precursor solution when reaching an equilibrium solution in the microdroplet. Like the case with water autoionization, the amounts of each species are determined based on the requirement that chemical equilibrium must be met everywhere in the microdroplet while maintaining stoichiometry.

The governing differential equation varies slightly depending on the nature of the species in the buffer as detailed in the section

Published under an exclusive license by AIP Publishing

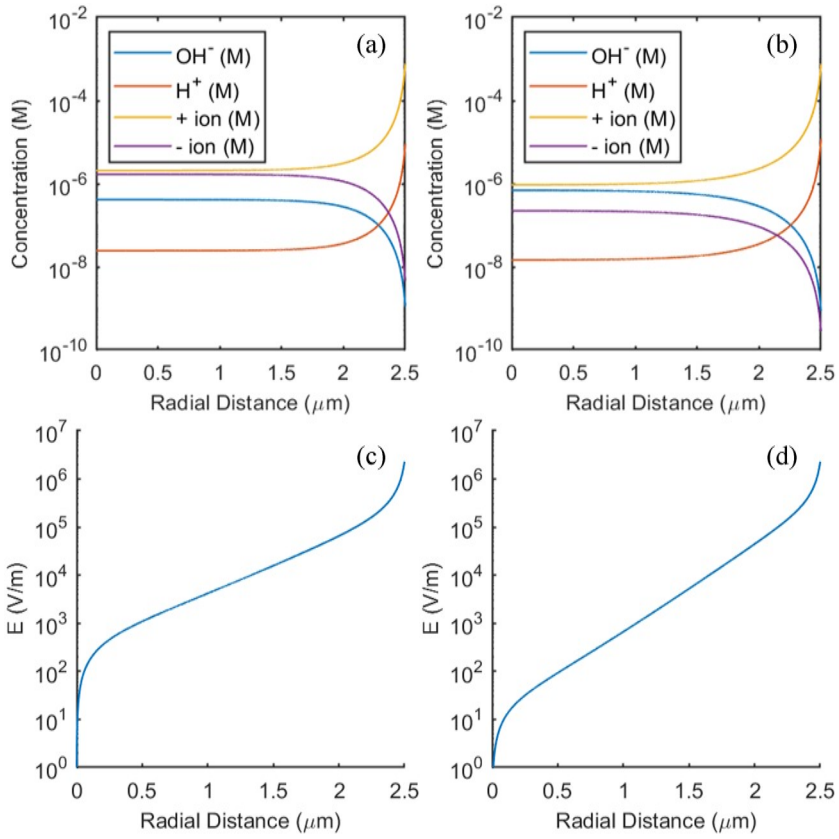

FIG. 2. Radial ion distributions (a) and (b) and radial electric field strength (c) and (d) in 5 μm diameter neutral aqueous microdroplets with a surface charge density of 0.01 ions per nm^2 at 25 °C. Internal ion average concentrations are as follows: (a) and (c) 100 nM negative strong electrolyte and 20.0 μM positive strong electrolyte and (b) and (d) 1 μM negative strong electrolyte and 20.9 μM positive strong electrolyte. The radial concentrations of the OH^- ion (blue), H^+ ion (red), positive strong electrolyte (yellow), and negative strong electrolyte (purple) are shown.

titled Calculations. Here, we demonstrate an example of a simple weak acid buffer solution, such as a buffer composed of acetic acid and sodium acetate. Consider a generic weak acid HA with acid dissociation constant, K_a,

$$HA \rightleftharpoons H^+ + A^-, \quad K_a = \frac{[H^+][A^-]}{[HA]}. \tag{9}$$

Instead of determining the boundary condition by conserving the total amount of HA and A^- in the microdroplet separately, the boundary conditions are determined by conserving the total sum of the moles of HA and A^- in the microdroplet and then enforcing the constraint of Eq. (9) at all locations in the microdroplet. There is a weak interaction between the dipole moment of neutral molecules and the divergence of the electric field. We have shown in our previous work[9] that this has a negligible effect on the distribution of neutral species in the microdroplet, and we approximate neutral species as having a constant concentration throughout the microdroplet.

The governing equation for a weak acid buffer is derived in the section titled Calculations at the end of this manuscript and incorporates the constraint in Eq. (9). The resulting governing equation is as follows:

$$\frac{1}{r^2}\frac{\partial}{\partial r}\left(r^2\frac{1}{[\mathrm{H}^+]}\frac{\partial[\mathrm{H}^+]}{\partial r}\right) = \frac{F}{V_T\,\varepsilon}\left\{(1+R_+)[\mathrm{H}^+] + (K_w + K_a[HA])/[H^+]\right\}, \tag{10}$$

where $[HA]$ is the concentration of weak acid in the microdroplet and is also an unknown parameter in the differential equation. Notably, it is not the same as the concentration of weak acid in the precursor solution used to form the microdroplet. Again, there are four boundary conditions as it is a second-order differential equation with two unknown parameters (R_+ and $[HA]$) as follows:

$$\nabla[H^+] = 0 \text{ at center of the droplet,} \tag{11}$$

$$\text{total surface charge} + \iiint_V \rho\, dV = \text{net droplet charge,} \tag{12}$$

$$\iiint_V c_+ dV = \text{moles of} + 1 \text{ ion in the droplet}\left(\text{excluding } \mathrm{H}^+\right), \tag{13}$$

and

$$\iiint_V (c_A + c_{HA})dV = \text{combined moles of acid and conjuagate base in droplet.} \tag{14}$$

Published under an exclusive license by AIP Publishing

The boundary condition in Eq. (14) conserves the sum of A^- and HA species as this is a known quantity in the microdroplet precursor solution and conserved in the transition to a microdroplet.

We solve the case of an acetic acid:sodium acetate buffer with a pK_a value of 4.756.[28] A careful examination of Eqs. (3) and (10) shows that they are the same when $K_w R_- = K_a[HA]$. In Fig. 2(b), we can substitute in the acetate ion for the strong negative electrolyte for the specific case when the concentration of acetic acid is 2.26 nM in the microdroplet. The precursor solution would consist of 19.9 μM SDS, 1 μM sodium acetate, and 2.26 nM acetic acid, with a pH of 9.69, which is well outside a useful pH range of this buffer.

It makes more sense to compare microdroplets from the precursor solutions of 19.9 μM SDS and 1 μM NaCl shown in Fig. 2(b) to a buffered solution of 19.9 μM SDS, 1 μM sodium acetate, and 1 μM acetic acid, which has a pH of 4.75, the optimal pH for an acetic acid:sodium acetate buffer. The ion distributions for this microdroplet are shown in Fig. 3 and are different from those in Fig. 2(b). Figure 3 provides an even more powerful example of how the moles of H^+ and OH^- are not conserved. The $-\log_{10}(\text{average}[H^+])$ and $-\log_{10}(\text{average}[OH^-])$ of the microdroplet are 6.0 and 7.3, respectively, with $-\log_{10}(\text{average}[H^+])$ ranging from 4.4 at the edge to 6.8 at the center. Note that despite the presence of the buffer, a strong radial $[H^+]$ gradient persists inside the microdroplet. Furthermore, this is not simply an increase in $[H^+]$ at the edge of the microdroplet. The center of the microdroplet at a $-\log_{10}(\text{average}[H^+])$ of 6.84 is shifted from the pH 4.75 of the buffered precursor solution, and the acetic acid concentration has shifted from 1 μM in the precursor solution to a mere 24.9 nM in the microdroplet. Most of the acetic acid has dissociated to form additional acetate ions needed to satisfy the EDL governing equation. Nonetheless, the chemical equilibria of both the buffer and water autolysis are met in all locations within the microdroplet. This demonstrates how different the environment within a microdroplet can be from its precursor solution.

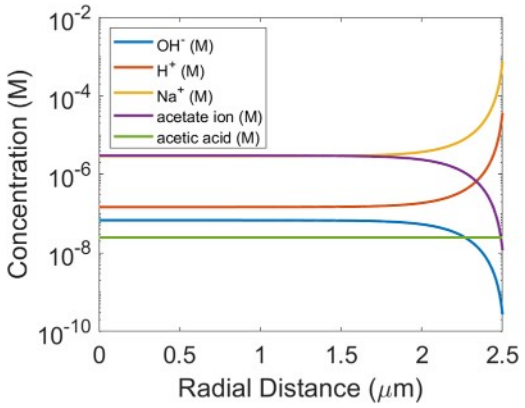

FIG. 3. Radial ion distributions in 5 μm diameter neutral aqueous microdroplets with a surface charge density of 0.01 ions per nm^2 at 25 °C, formed from a precursor buffer solution of 19.9 μM SDS, 1 μM sodium acetate, and 1 μM acetic acid. The radial concentrations of the OH^- ion (blue), H^+ ion (red), sodium ion (yellow), acetate ion (purple), and acetic acid (green) are shown.

The $[H^+]$ gradient in a microdroplet opens the possibility of acid or base catalyzed reactions being catalyzed in a microdroplet. Depending on the microdroplet buffer solution, it is possible to get microdroplets that contain both acidic and basic regions at the same time. Furthermore, the ion gradients can alter the net reaction rate in a microdroplet away from the reaction rate of the average concentrations. Of particular note are reactions with ions concentrated toward the surface (in the example case, positive ions) reacting with any surface-bound species, either neutral or charged.

Potential energy of charge separation in a microdroplet

The extent of charge separation within the microdroplet can be quantified by calculating the electrostatic potential energy of the ion configuration of the microdroplet. The electrostatic potential energy of the charge configuration (U_E) in a spherically symmetric microdroplet of radius R can be expressed as[29]

$$U_E = \frac{1}{2}\iiint_V \rho(r)\varphi(r)dV + \frac{1}{2}\oiint_s \sigma\varphi(R)dS, \tag{15}$$

where the two terms are an integral of the free charge density ρ times the potential φ over the volume of the microdroplet and the electric potential at the surface times the surface charge density σ, integrated over the surface of the microdroplet. Because we are concerned primarily with the change in potential energy, the location of the zero potential can be chosen arbitrarily for net-neutral microdroplets. Following our previous work,[9] we define the zero potential to be at the center of the microdroplet. For systems where the microdroplet has a net charge, more care must be taken with the location of zero potential, and $\varphi(\infty) = 0$ should be used.

Reaction pathways that can be driven by microdroplets

Having established the ion distributions in a microdroplet and quantified the resulting potential energy related to the charge separation in a microdroplet, we consider reaction pathways that alter the extent of charge separation in the microdroplet. There are a wide variety of such reaction pathways. One reaction pathway would be for a surface-bound ion (S^-) to oxidize a dissolved neutral species (N^0) to form a dissolved negative ion (N^-) and a neutral species (S^0). We refer to this process as the ion-to-ion reaction pathway,

$$S^- + N^0 \rightarrow S^0 + N^-.$$

This reaction pathway lowers the surface charge density of the microdroplet while increasing the number of dissolved negative ions

Published under an exclusive license by AIP Publishing

in the areas of the microdroplet with positive net charge density, thereby lowering the charge separation in the microdroplet.

Another reaction pathway would be for a surface-bound ion (S^-) to react with a dissolved positive ion (P^+) to form a neutral species (N^0). We refer to this as the ion-to-neutral reaction pathway,

$$S^- + P^+ \rightarrow N^0.$$

This reaction pathway lowers the surface charge density of the microdroplet while also lowering the number of dissolved positive ions in the areas of the microdroplet with positive net charge density. This also lowers the charge separation in the microdroplet.

There are other less intuitive reaction pathways that lower the charge separation, for example, a reaction that takes two univalent dissolved positive ions (P^+) and combines them into a divalent dissolved positive ion (P^{2+}),

$$P^+ + P^+ \rightarrow P^{2+}.$$

The increase in the valence of the ions composing the EDL shifts the ion distribution in the EDL. The areas of positive net charge density are compressed toward the edge of the microdroplet by this change in ion valence. This effectively brings the regions of negative and positive net charges closer to each other, and thus, this reaction pathway lowers the charge separation in the microdroplet. This is by no means an exhaustive list. It can get immensely more complex if reactions that form weak electrolytes and the following cascade of interrelated chemical equilibria are considered. Note that different reaction pathways may experience different driving forces as they do not affect the charge separation of the microdroplet in the same manner.

Microdroplet driving force on an ion-to-ion reaction pathway

We concern ourselves primarily with the ion-to-ion reaction pathway where a surface bound ion oxidizes a dissolved neutral species to form a dissolved negative ion and a neutral species. At a very fundamental level, an applied voltage to a reaction can be expressed as the change in the potential energy of the macroscopic system (U) per unit of charge transferred in the reaction, omitting the thermodynamics of the specific reaction itself. The thermodynamics of the specific reaction are omitted as we calculate the additional driving force supplied to the reaction from the system. The applied voltage (V) can be expressed mathematically as a partial derivative of the potential energy of U per coulomb of charge transferred by the reaction (c_{rxn}) along the path of the reaction,

$$V = \left.\frac{\partial U}{\partial c_{rxn}}\right|_{along\ reaction\ path}. \tag{16}$$

For the ion-to-ion reaction, the moles of surface-bound ions (N_S) are decreased with a corresponding increase in the moles of internal strong electrolyte negative ions (N_N); meanwhile, both the moles of the strong electrolyte (N_P) and the sum of moles of surface-bound ions (N_S) and strong electrolyte negative ions (N_N) in the microdroplet are held constant. The moles of H^+ and OH^- are allowed to vary in accordance with the equilibrium constant of water

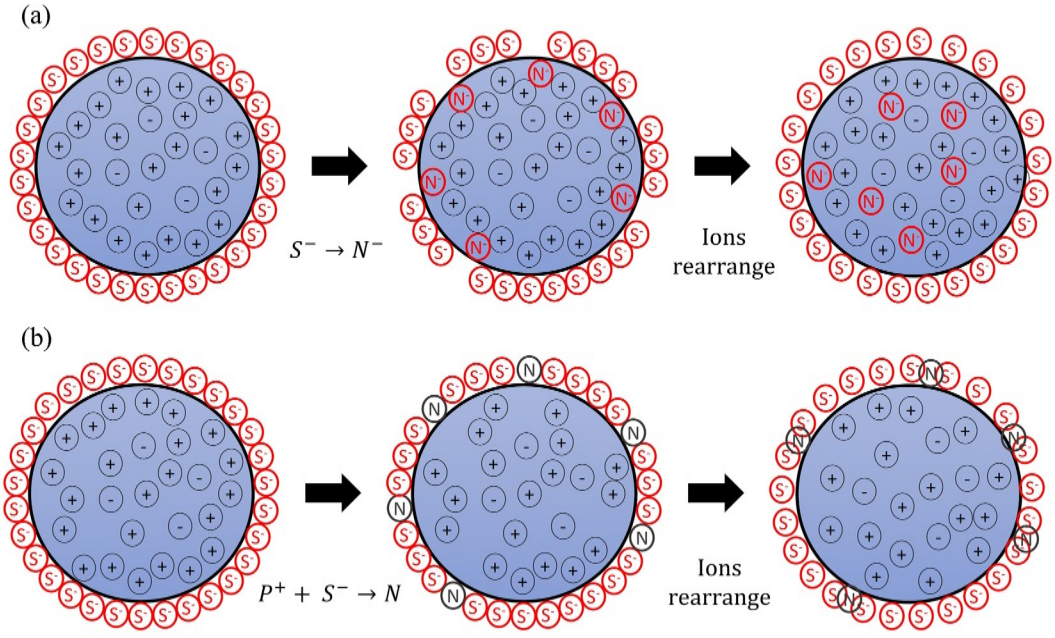

FIG. 4. Illustrations of two adiabatic reaction pathways: (a) ion-to-ion reaction pathway and (b) ion-to-neutral reaction pathway. In both figures, we have assumed that the surfactant is negatively charged, but this choice is arbitrary, as explained in the text.

Published under an exclusive license by AIP Publishing

and EDL considerations,

$$V = \left.\frac{\partial U}{\partial N_S}\right|_{N_P,(N_S+N_N)}. \tag{17}$$

We recently used the same methodology on a similar case involving a planar surface as opposed to a microdroplet.[30] In that one-dimensional case, the potential energy of an EDL was used to drive a reaction, wherein a static charge on a surface was imparted to the liquid via a redox reaction. This one-dimensional case was solved analytically for U, and then, the derivative of U with respect to the surface charge density was used to calculate the voltage.

Unfortunately, we do not have an analytical solution for U for spherical microdroplets. We treat the reaction as an adiabatic process, wherein the reaction is slow relative to the microdroplet reestablishing its EDL equilibrium. This allows us to consider the reaction in a stepwise manner as depicted in Fig. 4. First, the potential energy of the microdroplet in its equilibrium EDL is calculated, the ion amounts in the microdroplet are adjusted along the reaction pathway, and the potential energy of the microdroplet in its equilibrium EDL with the changed ion concentrations is calculated. This is repeated with small steps along the reaction pathway to estimate the derivative of U and thus determine the voltage. Again, the thermodynamics of the specific reaction are omitted from the calculation of U as we calculate the additional driving force supplied to the reaction from the microdroplet.

Figure 5 shows the change in the number of ions within the microdroplet over the course of the ion-to-ion reaction pathway for the same two microdroplets as in Fig. 2. As per the specifications of the ion-to-ion reaction, the amount of positive strong electrolytes remains unchanged by the reaction, and surface-bound ions are converted to negative strong electrolyte ions stoichiometrically. Interestingly, however, the count of H^+ ions and OH^- ions is not constant. Instead, we observe the recombination of H^+ and OH^- ions coupled to the reaction via the EDL.

It is important to recall at this point that the moles of H^+ and OH^- are allowed to vary in accordance with the equilibrium constant of water and EDL considerations, and their amounts are not necessarily fixed along the reaction pathway. The recombination of OH^- and H^+ provides another source of potential energy, in this case chemical potential energy (U_{chem}), which becomes coupled to the ion-to-ion reaction through the EDL of the microdroplet. Like the electrostatic potential energy, we are interested in the change in this potential energy as the reaction takes place so the zero potential can be chosen arbitrarily. We define zero potential as if every mole of OH^- reacted to form water and the coupled chemical potential

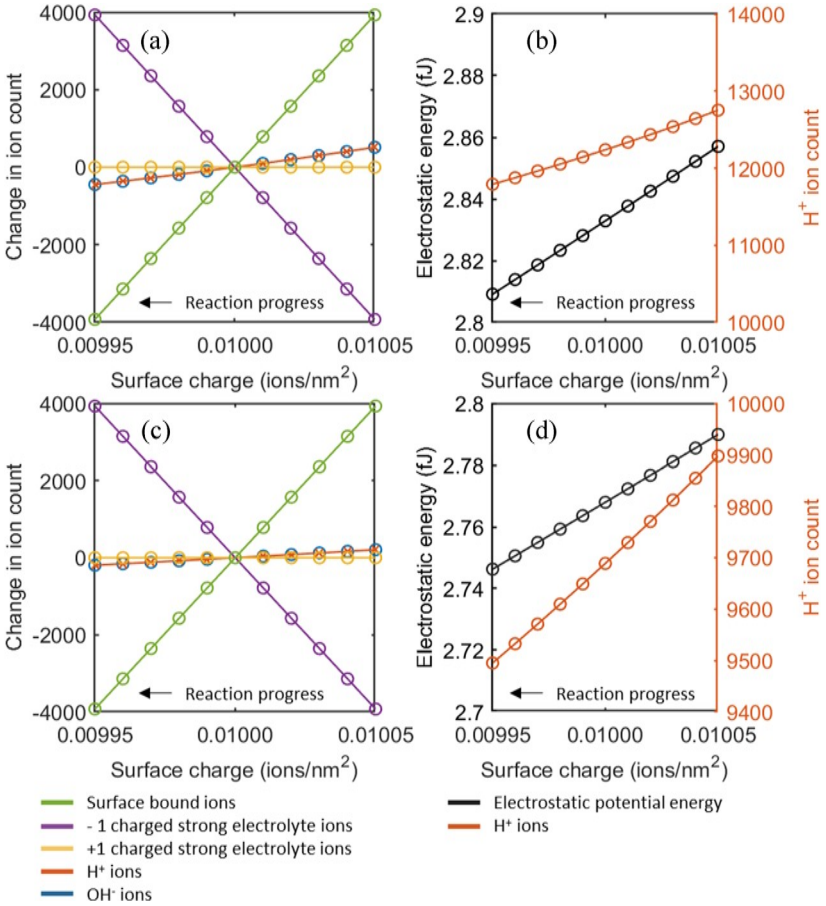

FIG. 5. Change in the ion count as a reaction takes place that converts surface ions to strong univalent negative electrolyte ions for 5 μm diameter neutral aqueous microdroplets with an initial surface charge density of 0.01 ions per nm^2. Initial internal ion average concentrations are as follows: (a) and (b) 100 nM negative strong electrolyte and 20.0 μM positive strong electrolyte and (c) and (d) 1 μM negative strong electrolyte and 20.9 μM positive strong electrolyte. (a) and (c) show the change in ion counts for surface-bound ions (green), OH^- ions (blue), H^+ ions (red), positive strong electrolyte (yellow), and negative strong electrolyte (purple). (b) and (d) show the electrostatic potential energy of the EDL (black) and the total count of H^+ ions in the microdroplet (red).

Published under an exclusive license by AIP Publishing

energy as the product of the moles of OH^- and the enthalpy of water recombination,

$$U_{chem} = N_{OH} x \Delta H_{water}. \quad (18)$$

Here, ΔH_{water} is the enthalpy in Joules per mole of the recombination of OH^- and H^+ to form water and N_{OH} is the total moles of OH^- in the microdroplet. The chemical potential energy for other chemical equilibria that are present in the microdroplet can be included in a similar manner. The change in U_{chem} over the course of the main reaction contributes an effective voltage, V_{chem}, owing to the coupling between the two reactions caused by the microdroplet EDL. As expected, the electrostatic potential energy (U_E) of the microdroplet changes as the reaction takes place, as shown in Figs. 5(b) and 5(d). This change in potential energy as the reaction occurs contributes an effective voltage, V_{elec}. Table I summarizes the effective voltages from these two processes. The macroscopic potential energy of the microdroplet is then simply the sum of the electrostatic potential energy and the coupled chemical potential energy,

$$U = U_E + U_{chem}. \quad (19)$$

The observed decrease in effective voltage as the ion concentration increases within the microdroplet is expected. In the limit of high ion concentrations, the EDL becomes thin relative to the diameter of the microdroplet, and the behavior of the system returns to that of a bulk solution with a very thin double layer at the surface.

As previously mentioned, many different reactions are possible. For example, a redox reaction could form a weak electrolyte that goes on to react further with a different chemical equilibrium within the microdroplet. In each case, a gradient of U can be taken that preserves the appropriate ion conservations given by the stoichiometry of the reactions involved. This gradient will vary as per the specifics of the reaction under consideration. The calculations as presented below include options for calculating numerically the U value of a droplet for any solvent, either sign for the surface charge, any net charge on the droplet, and with or without weak electrolytes, such as buffers. Furthermore, it includes options for multivalent ions. Most chemical reactions in microdroplets can be expressed within this framework.

TABLE I. Ion-to-ion reaction driving force on 5 μm diameter neutral aqueous microdroplets with a surface charge density of 0.01 ions per nm^2. Internal ion average concentrations are the 100 nM negative strong electrolyte and 20.0 μM positive strong electrolyte for droplet (a) and 1 μM negative strong electrolyte and 20.9 μM positive strong electrolyte for droplet (b). r^2 is the coefficient of determination for the fit of the points displayed in Figs. 5(b) and 5(d).

Droplet	Salt concentration	Voltage source	Voltage (mV)	r^2
(a)	100 nM	V_{chem}	73.0	(0.998 544)
		V_{elec}	38.1	(0.999 981)
		V_{total}	111	(0.999 293)
(b)	1 μM	V_{chem}	30.6	(0.999 606)
		V_{elec}	34.6	(0.999 994)
		V_{total}	65.2	(0.999 888)

Microdroplet reaction driving force changes along an ion-to-ion reaction pathway

As one would expect, the driving force on the reaction falls off as the reaction progresses, assuming that surface-bound S^- ions are not replenished from the medium surrounding the microdroplet. During the reaction, the surface charge decreases and the ionic strength inside the microdroplet increases. Both decrease the driving force on the reaction. The graph terminates very close to the highest possible surface charge density for the stated reactant concentrations. Along the course of the reactions shown in Fig. 6(a), the following remain fixed: diameter of 5, 20.0 μM positive strong

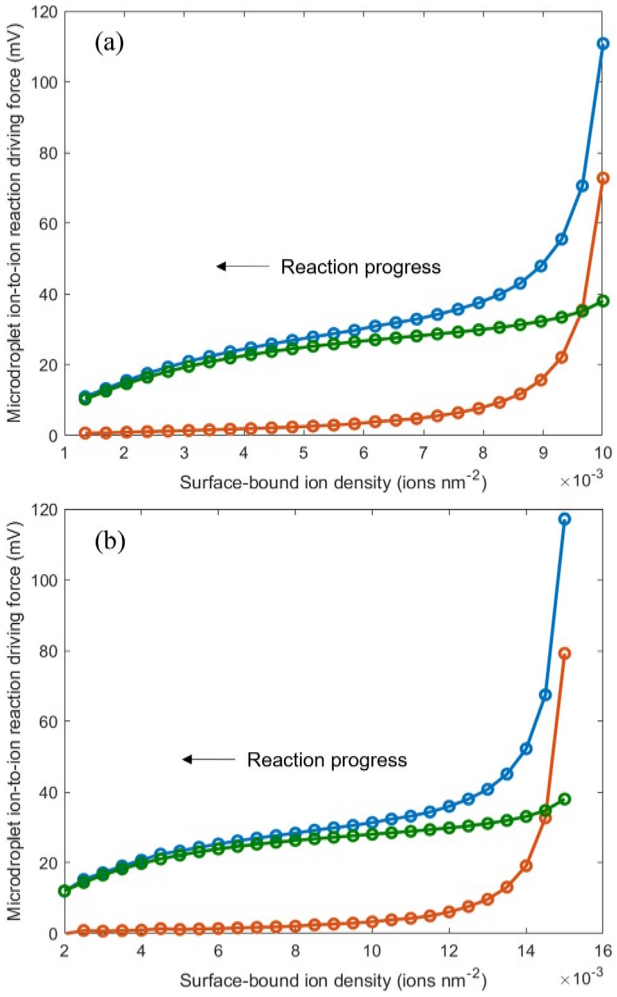

FIG. 6. Microdroplet driving force along an ion-to-ion reaction pathway: total driving force (blue, mV), electrostatic contribution (green, mV), and water recombination contribution (red, mV). The microdroplet remains constant at 5 μm diameter and 25 °C. Ions are conserved according to the reaction stoichiometry and water recombination stoichiometry. Initial parameters at the start of reaction are as follows: (a) 0.010 ions per nm^2 surface charge, 100 nM negative strong electrolyte, and 20.0 μM positive strong electrolyte and (b) 0.015 ions per nm^2 surface charge, 100 nM negative strong electrolyte, and 30.0 μM positive strong electrolyte.

Published under an exclusive license by AIP Publishing

electrolyte, and all other ions are conserved according to the reaction stoichiometry and water recombination stoichiometry. Under these conditions, the highest possible surface charge density, reached when the negative strong electrolyte is 0 M, is 10.05×10^{-3} ions per nm^2. Obviously, higher surface charge densities are possible, but they require different concentrations of species in the microdroplet and thus have different voltages as the surface is discharged from the example depicted in Fig. 6(a).

A similar example of a reaction starting from a higher surface charge density microdroplet is shown in Fig. 6(b). In this example, again the diameter is fixed at 5 μm and ions are conserved according to the reaction stoichiometry and water recombination stoichiometry. However, the positive strong electrolyte is at 30.0 μM to maintain a net charge neutral microdroplet overall. When this microdroplet reaction has progressed down to 0.010 ions per nm^2, where Fig. 6(a) starts, there is a significantly higher concentration of salt within the microdroplet than the case shown in Fig. 6(a), which causes a significantly different reaction driving force.

Interestingly, the contribution from recombination at first dominates the reaction and then quickly falls off as the negative electrolyte is formed by the reaction. Comparing Figs. 6(a) and 6(b), while the driving force is increased by the increased surface charge density, the water recombination contribution to the behavior of driving force seems to be far more sensitive to a low concentration of the negative strong electrolyte as opposed to the specific surface charge. The increase in voltage when a product species is in low concentration is reminiscent of the half-cell voltage calculated from the Nernst equation from which an infinite voltage is calculated for the limit of no initial product. This is also why we do not calculate the microdroplet case containing no negative strong electrolyte.

Microdroplet reaction driving force changes along the ion-to-neutral reaction pathway

For the surface charge recombination reaction pathway, a surface-bound ion reacts with a dissolved positive ion to form a neutral species. The stoichiometry of the reaction maintains a fixed difference between the moles of the strong electrolyte (N_P) and moles of surface-bound ions (N_S); meanwhile, the moles of strong electrolyte negative ions (N_N) are held constant. Again, the moles of H^+ and OH^- are allowed to vary in accordance with the equilibrium constant of water and EDL considerations. Equation (16) can be expressed with these conditions as follows:

$$V = \left.\frac{\partial U}{\partial N_S}\right|_{N_N,(N_P-N_S)}. \tag{20}$$

This reaction pathway is illustrated in Fig. 4(b). Again, we treat the reaction as an adiabatic process, wherein the reaction is slow relative to the microdroplet reestablishing its EDL equilibrium. This allows us to consider the reaction in a stepwise manner as depicted in Fig. 4(b). First, the potential energy of the microdroplet in its equilibrium EDL is calculated, the ion amounts in the microdroplet are adjusted along the reaction pathway, and the potential energy of the microdroplet in its equilibrium EDL with the changed ion concentrations is calculated. This is repeated with small steps along the reaction pathway to estimate the derivative of U and thus determine the voltage. The thermodynamics of the specific reaction are omitted from the calculation of U as we calculate the additional driving force supplied to the reaction from the microdroplet.

Figure 7 depicts an ion-to-neutral reaction starting from the same microdroplet as is depicted in Fig. 2(a) whose ion-to-ion reaction pathway is shown in Fig. 6(a). Note that the two reaction pathways experience different driving forces from the microdroplet. As the surface is discharged, the contribution from the electrostatic potential energy portion drops. Rather unintuitively, the contribution from the water recombination increases as the surface charge decreases until sharply dropping off at low surface charge densities. Unlike in the ion-to-ion reaction case, where the increase in strong electrolytes leads to an initially large amount of recombination of the acidic and basic portions of the microdroplet, in the ion-to-neutral reaction case, the reaction decreases the moles of strong electrolytes in the microdroplet, inhibiting the recombination of acidic and basic portions of the microdroplet over the course of the reaction. Eventually, the drop in surface charge overcomes the decrease in strong electrolytes and the acidic and basic portions recombine (large contribution at this point) and then the water recombination contribution to the driving force decreases sharply once the microdroplet no longer has a significant $[H^+]$ gradient. This illustrates the complexity of reactions taking place inside a microdroplet.

Microdroplet reaction driving force dependence on the microdroplet radius

The size of the microdroplet can have a large effect on the resulting voltage. Comparisons of microdroplets with the same

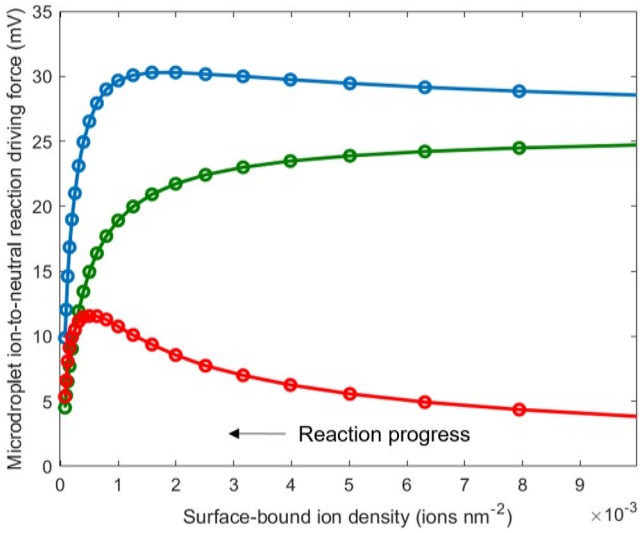

FIG. 7. Microdroplet driving force along an ion-to-neutral reaction pathway: total driving force (blue, mV), electrostatic contribution (green, mV), and water recombination contribution (red, mV). The microdroplet remains constant at 5 μm diameter and 25 °C. Ions are conserved according to the reaction stoichiometry and water recombination stoichiometry. Initial parameters at the start of reaction are as follows: 0.010 ions per nm^2 surface charge, 100 nM negative strong electrolyte, and 20.0 μM positive strong electrolyte.

Published under an exclusive license by AIP Publishing

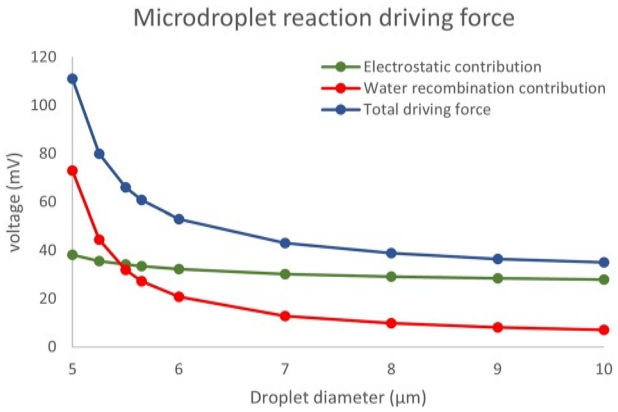

FIG. 8. Microdroplet driving force on an ion-to-ion reaction from microdroplets of different diameters with a surface charge of 0.01 ions per nm^2 made from precursor solutions with ionic strength and pH values as detailed in Table II. Shown are the total driving force (blue, mV), electrostatic contribution (green, mV), and water recombination contribution (red, mV).

surface charge density but different diameters are complicated by several factors. Unlike a traditional EDL, microdroplets lack a bulk solution to use as the reference for comparing the microdroplets of the same ionic strength and [H^+]. For the following comparison between microdroplets of different sizes, we consider microdroplets wherein the precursor bulk solution is of the same ionic strength and pH. Importantly, we neglect any contribution of the surfactant species of the microdroplet to the ionic strength of precursor solution. A further challenge is the variation in the counterion concentration with the microdroplet diameter. The number of surface ions, and thus corresponding dissolved counterions, scales with the radius squared, whereas the volume of the microdroplet scales with the radius cubed. To address this issue, we maintain the ionic strength of precursor solution by first including the necessary surfactant concentration to give the surface charge density and then varying the concentration of the dissolved strong electrolyte salt in the microdroplet precursor. Notably, this places a lower bound on the radii that can be used for a given ionic strength and surface charge density. A minimum radius is reached where the counterion concentration alone exceeds the desired ionic strength. In the example shown in Fig. 8, a diameter of 4.9 μm is impossible for the given ionic strength and surface charge density. The resulting precursor solutions for the microdroplets in Fig. 8 are given in Table II.

As a microdroplet increases in size, the driving force on the chemical reaction quickly drops off. This is the expected result, as in the limit of the large radius, the microdroplet should return to the same behavior as a bulk solution. For the electrostatic portion of the driving force, it returns to the limit of one thermal volt (25.7 mV at 25 °C) for a planar surface discharging an electrostatic charge. We have discussed this limit in a previous publication.[30] Figure 8 provides a rationale for why the microdroplet radius and spherical geometry play a crucial role in microdroplet chemistry beyond simply providing a high surface area environment. Many other mechanisms in microdroplets depend linearly on the surface area to volume ratio, which has a 1/R dependence on the droplet radius.[5,31] Here, the dependence on energy in the EDL, which depends nonlinearly on the surface area to volume ratio, causes the observed reaction driving forces to not follow this 1/R trend.

DISCUSSION

Extrapolation to higher surface charge densities

In an electrochemical cell, the electrostatic potential energy is discharged to drive a chemical reaction. The electrostatic potential energy is supplied by an external voltage power supply. In a microdroplet, we see the electrostatic potential energy of the microdroplet EDL acting as the "power supply" to drive a chemical reaction. Consequently, we consider microdroplets to act like an electrochemical cell. In the case with the largest driving force that we considered, the driving force was 111 mV. This value is quite modest from the viewpoint of electrochemical reactions. However, a surface charge density of only 0.01 charges per nm^2 was used to calculate this result, which is a quite low surface charge density. We therefore suspect that in many instances, the driving force of a reaction in a microdroplet may be higher. This speculation is further supported by the expected breakdown of the continuum model at the surface periphery.

TABLE II. Precursor solutions used to compare microdroplets of different diameters. Precursor solutions used to compare microdroplets of different diameters in Fig. 8.

Diameter (μm)	Surface charge density (ions per nm^2)	Counterion concentration (μM)	Salt concentration (nM)	Ionic strength (μM)	pH
5	0.01	19.93	100	10.0635	7
5.25	0.01	18.98	574	10.0635	7
5.5	0.01	18.12	1006	10.0635	7
5.75	0.01	17.63	1246	10.0635	7
6	0.01	16.61	1761	10.0635	7
7	0.01	14.23	2947	10.0635	7
8	0.01	12.45	3836	10.0635	7
9	0.01	11.07	4528	10.0635	7
10	0.01	9.96	5082	10.0635	7

Published under an exclusive license by AIP Publishing

Unfortunately, the differential equation involved in this work is rather stiff and becomes increasingly difficult to solve at higher surface charge densities. Furthermore, this model is the derivative from the one-dimensional Gouy–Chapman model, which is known to breakdown at higher surface charge densities owing to the dilute assumption of the ion flux equations. This can be corrected by the inclusion of a Stern layer near the surface followed by a diffuse portion of the EDL. The diffuse portion can then be modeled as in this paper with the Stern layer considered part of the atomic surface layer. However, such a treatment would not include the potential energy of the Stern layer itself in the model. We suggest using a more complex EDL model to account for such effects as a promising avenue for future work. The present study does demonstrate the existence of these driving forces and indicates how they sensitively depend on the microdroplet size and species concentrations, including those that might have been naively thought of as inert spectator ions that do not affect reactions in the microdroplet.

Despite the stiffness of the governing equation, we were able to calculate the resulting ion distributions and voltage of a 1 ion per nm^2, 5 μm diameter microdroplet as shown in Fig. 9. As can be seen, the strong positive electrolyte species is predicted to have a concentration of 7.45 M. This lies outside the dilute ion flux assumption made in the calculation. A similar failure of the one-dimensional Gouy–Chapman model is well known for cases with high surface charge densities. It is indicative of the formation of a Stern layer in the EDL.

Neglecting the issue of high concentrations, the microdroplet driving force is only slightly higher than the lower surface charge density microdroplets previously shown. The total driving force is 169 mV ($r^2 = 0.999\,305$), with the electrostatic component contributing 32 mV ($r^2 = 0.999\,997$) and the water recombination component contributing the other 137 mV ($r^2 = 0.998\,941$). While the driving force remains similar, the amount of electrostatic energy stored in the microdroplet EDL at 322 fJ is roughly two orders of magnitude higher than that of similar microdroplets with two orders of magnitude lower surface charge density.

Size effects on microdroplet chemistry

The chemistry in the microdroplet is quite sensitive to the size of the microdroplet. If the microdroplet is too big, the system returns to a case of a one-dimensional planar interface and the driving force is too small to exert much effect. If the microdroplet is too small, the charges are not sufficiently separated to store significant amounts of energy. Thus, there is an optimum size range for microdroplet chemistry that is driven by these effects. This makes microdroplet chemistry unique from both bulk chemistry and cluster chemistry. The defining features of the size range are the significant depletion of oppositely charged ions to the surface charge and accumulation of similarly charged ions to surface charge at the center of the microdroplet.

It is tempting to imagine that accelerated chemical reactions observed in microdroplets occur only from the partial solvation of the species at its surface. If this were the case, microdroplets of different sizes but the same surface concentrations of reactants should all exhibit the same reaction rate. These reactions would be observed on the surfaces of dilute bulk solutions, which is not the case. Consequently, while partial solvation is certainly important in the chemistry of microdroplets, more must exist to this story. We suggest that the electric field arising from the EDL and the mechanism presented here, which adds an additional driving force, may make important contributions to the origins of accelerated reactions in microdroplets in some cases.

Limitations of the model

Our work relies on a continuum model. Continuum models are extremely useful in allowing calculus to be applied to a system of discrete charges. With continuum models, one should be cautious to double check that the concentrations still represent enough particles that their time-averaged motion acts in a continuum manner. For smaller microdroplets, an atomistic approach is to be preferred.[32] For example, consider a water microdroplet with a volume of 1 fL and an average $[H^+]$ of 10^{-9} M. Simple geometry will show the diameter to be 1.24 μm,

$$1\,fL = 4\pi r^3/3, \tag{21}$$

$$r = 0.620\,\mu m. \tag{22}$$

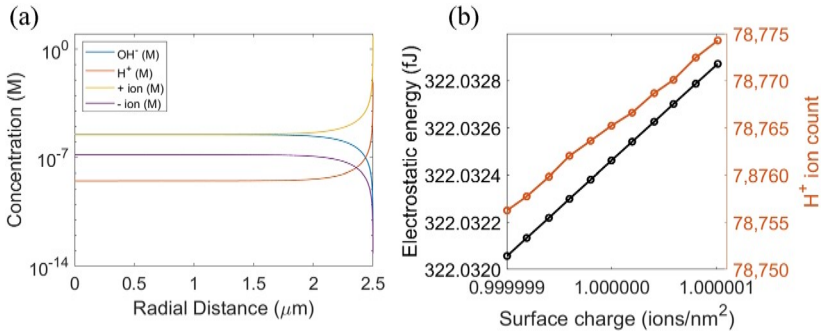

FIG. 9. Neutral aqueous microdroplets of 5 μm diameter with a surface charge density of 1 ion per nm^2. Internal ion average concentrations are the 100 nM negative strong electrolyte and 20.0 μM positive strong electrolyte. (a) Radial concentrations of the OH^- ion (blue), H^+ ion (red), positive strong electrolyte (yellow), and negative strong electrolyte (purple). (b) Electrostatic potential energy of the EDL (black) and the total count of H^+ ions in the microdroplet (red).

Published under an exclusive license by AIP Publishing

This, while small, is still within the range of microdroplet sizes we are interested in. If we calculate the total moles of the H^+ ion within the microdroplet, we obtain 10^{-24} mol. Using Avogadro's number, we find a total of 0.6022 molecules of the H^+ ion. Obviously, we cannot have a fractional count of molecules in the microdroplet. In the case of the H^+ ion, this represents that 60% of the time, a molecule of H^+ exists within the droplet. Obviously, the electric field generated by a single H^+ ion that only exists 60% of the time is not going to be well represented by a continuum model for the ion distribution in the microdroplet. This is danger that we need to remain aware of when working in a continuum model. Similarly, for a 1 fL microdroplet containing an average $[H^+]$ of 10^{-9} M, the count of OH^- ions effectively disappears from the system.

We are aided by geometry, as the volume of the microdroplet scales as the cube of the diameter. Thus, a 12.4 μm diameter microdroplet has a volume of 1 pL and, if we assume an average $[H^+]$ of 10^{-9} M, there are 602 molecules of H^+, which is well approximated by a continuum model. Conversely, applying continuum models to nanodroplets should be done with great care as the ion count problem becomes significantly worse at that scale.

There are a few technical notes related to the derivation. We approximate that dielectric strength (ε), water autoionization constant (K_w), and other chemical equilibrium constants are all independent of the electric field strength. A missing element in this model is changes in the entropy of the microdroplet. In addition to changes in the potential energy of the system, there are also changes in entropy related to the confinement of ions into the EDL. The changes in entropy as the EDL changes the shape are not currently accounted for and present an interesting avenue for future work.

Finally, it should be recognized that this model is incomplete in describing the full breadth of reaction mechanisms in a microdroplet. We fail to treat the several layers of molecules at the interface of the microdroplet, rather than to assign them a two-dimensional surface charge density. Reactions occurring in this periphery layer experience effects related to the atomistic environment, such as the orientation of solvent molecules at that interface, the partial solvation of reactants, and the electric field effect in altering the dielectric constant and equilibrium constants. For example, see works done by Narendra and co-workers,[3] Hao and co-workers,[4] and others.[33,34] Thus, our treatment may actually be an underestimate of the driving forces that accelerate reactions in microdroplets.

CONCLUSION

A water microdroplet EDL stores potential energy both electrostatically and chemically by altering other internal chemical equilibria of the microdroplet. This stored potential energy can be utilized to drive chemical reactions, much like an electrochemical cell. Energy is stored electrostatically in both ion gradients in the EDL and the $[H^+]$ gradient and any chemical equilibrium of ions within the microdroplet. As reactions progress in the microdroplet, these additional sources of energy couple and drive the reaction. Of note is the energy gained by the recombination of H^+ and OH^- across the microdroplet. This provides the major contribution to the calculated effective voltage for the ion-to-ion reaction pathway. These microdroplet driving forces on reactions within them are particularly sensitive to the size of the microdroplet and cause chemistry to occur that is unique to microdroplets as opposed to bulk solution or nanoclusters.

Calculations

The distribution of species in a microdroplet is derived from ion conservation and Gauss's law. The concentrations of all ion species are rewritten into functions of the H^+ ion concentration, resulting in a second-order differential equation that is solved numerically to calculate the EDL. Finally, a pseudo-steady-state condition is used to calculate the driving force on a reaction using a series of microdroplet EDL configurations following the stoichiometry of the chemical reaction of interest.

Ion conservation

The ion conservation equation includes a divergence of the Nernst–Planck flux $\vec{j}_i$ and a chemical reaction source term R_i,[35]

$$\frac{\partial c_i}{\partial t} = -\nabla \cdot \vec{j}_i + R_i. \tag{23}$$

Here, c_i is the local concentration of the ith species (mole m^{-3}), t is the time (s), $\vec{j}_i$ is the flux of the ith species (mole m^{-2} s^{-1}), and R_i is the net local reaction rate of the ith species (mole m^{-3} s^{-1}). The steady-state solution is defined by $\partial c_i/\partial t = 0$. The Nernst–Planck flux is written as the sum of three terms, bulk motion ($c_i\vec{u}$), electromigration ($\mu_i F z_i c_i \nabla\varphi$), and a (dilute system) diffusion flux ($D_i \nabla c_i$),[36] which is a commonly used approximation based on infinite dilution,

$$\vec{j}_i = c_i\vec{u} - \mu_i F z_i c_i \nabla\varphi - D_i \nabla c_i. \tag{24}$$

Here, μ_i is the ion mobility (mol m^2 V^{-1} s^{-1} C^{-1}), F is Faraday's constant (C mol^{-1}), z_i is the ion charge (unitless but signed), φ is the electric potential (V), and D_i is the diffusion coefficient (m^2 s^{-1}).

We assume a microdroplet that is at pseudo-chemical equilibrium (all species except the slow reaction of interest at equilibrium). This dictates that $R_i = 0$ everywhere within the microdroplet. For those with concerns about buffers interacting with $[H^+]$ gradients inside EDLs, we have previously shown that for systems following a Boltzmann distribution of ions (as is true in this case), chemical equilibrium is achieved throughout the EDL.[24] This includes $[H^+]$ gradients inside EDLs being stable despite the presence of a buffer.

We also assume that the bulk liquid in the microdroplet does not move in the reference frame of the droplet, $\vec{u} = 0$, thereby eliminating the first term in Eq. (24). We further simplify Eq. (24) by using the Nernst–Einstein equation,[37] which relates the diffusion coefficient and ion mobility via a temperature-dependent constant (with units of electric potential), known as the thermal voltage V_T,

$$V_T = \frac{D_i}{\mu_i F} = \frac{k_b T}{e}. \tag{25}$$

This leaves behind a very simple ion conservation law for the microdroplets,

$$-z_i c_i \nabla\varphi = V_T \nabla c_i. \tag{26}$$

Published under an exclusive license by AIP Publishing

Note that integrating Eq. (27) gives a familiar Boltzmann distribution of ions as follows:

$$c_i = c_i^0 \exp(-z_i\varphi/V_T), \tag{27}$$

where c_i^0 is the concentration of the ith ion in the center of the microdroplet.

Next, we consider the differential form of Gauss's law as follows:

$$\nabla \cdot (\varepsilon \nabla \varphi) = -\rho, \tag{28}$$

where ρ is the local charge density (Cm^{-3}) and ε is the dielectric constant (F m^{-1}). Replacing $\nabla\varphi$ using Eq. (26), we obtain

$$\nabla \cdot \left(\varepsilon \frac{V_T \nabla c_i}{z_i c_i}\right) = \rho. \tag{29}$$

Up to this point, the equations are general with regard to the shape of the system. We now assume a spherical droplet in which c_i depends only on the radial distance (r).

Converting to spherical coordinates and assuming that ε is a scalar whose value is independent of the electric field strength, we find

$$\frac{1}{r^2}\frac{\partial}{\partial r}\left(r^2 \frac{1}{c_i}\frac{\partial c_i}{\partial r}\right) = \frac{z_i \rho}{\varepsilon V_T}. \tag{30}$$

Charge density expansion

We expand the local charge density in terms of the ion concentrations as follows:

$$\rho = \sum_i^{all\ spesies} F z_i c_i. \tag{31}$$

Next, we write all other species concentrations as functions of the H^+ ion concentration, $[H^+]$, in the microdroplet. We previously stated that the steady-state solution of the system has all locations at chemical equilibrium. As such, we can relate the concentrations of H^+ and OH^- via the equilibrium constant of water (K_w) as follows:

$$\left[OH^-\right] = K_w/\left[H^+\right]. \tag{32}$$

A similar equation can be written for weak acids and bases. We approximate neutral species as having a single concentration throughout the droplet. Our previous work[9] has shown that the effect of the divergence of the electric field in a microdroplet on the dipole of a neutral molecule can be neglected. For example, the concentration of a generic weak acid (HA) and its conjugate base (A^-) can be expressed in terms of the H^+ concentration as follows:

$$\left[A^-\right] = K_a[HA]/\left[H^+\right]. \tag{33}$$

Multiproteic acids and bases can be written as functions of H^+ concentration, equilibrium constants, and neutral species by combining the equilibrium constant equations of the various deprotonation steps.

Finally, we need to address strong electrolyte species, which, by their nature, do not have equilibrium constants with H^+ ions. Ions of the same valence have the same ratio at all points within the microdroplet. Let us start with +1 charged species. Taking the ratio of the species and H^+ ion concentrations and substituting in the Boltzmann equation shown in Eq. (27), we obtain

$$\frac{c_i}{[H^+]} = \frac{c_i^0 \exp[-\varphi/V_T]}{[H^+]_c \exp[-\varphi/V_T]} = \frac{c_i^0}{[H^+]_c} = R_+. \tag{34}$$

Here, $\left[H^+\right]_c$ is the H^+ concentration at the center of the microdroplet. The value of R_+ is an unknown parameter in the differential equation and is determined by the boundary conditions. Rearranging Eq. (34), we obtain

$$c_i = R_+\left[H^+\right] \text{ for } z_i = +1, \tag{35}$$

which can be used to simplify the governing differential equation by replacing +1 charged ions with a dependence on the concentration of $[H^+]$.

Similarly, for −1 charged species, taking the ratio of the species and OH^- ion concentrations and substituting in Eq. (27) yield a constant ratio throughout the microdroplet as follows:

$$\frac{c_i}{[OH^-]} = \frac{c_i^0 \exp[-\varphi/V_T]}{[OH^-]_c \exp[-\varphi/V_T]} = \frac{c_i^0}{[OH^-]_c} = R_-, \tag{36}$$

where $\left[OH^-\right]_c$ is the concentration of OH^- at the center of the microdroplet. Relating $[OH^-]$ to $[H^+]$ gives the following that can be used to simplify the following governing equation:

$$c_i = R_- K_w/[H^+] \text{ for } z_i = -1. \tag{37}$$

Once again, the value of this ratio, R_-, is an unknown parameter in the differential equation and is determined by the boundary conditions. For systems with strong electrolyte ions of larger valences, if a weak electrolyte ion of the same valence has been already written as a function of $[H^+]$, then a ratio can be constructed. If this is not the case, then a system of differential equations must be constructed as we have done previously.[9]

In this work, the saltwater examples are systems containing H^+, OH^-, and two strong electrolytes of +1 and −1, respectively. For these systems of ions, expanding Eq. (31) and using the substitutions from Eqs. (32), (35), and (37) give the following:

$$\rho = F(1 + R_+)\left[H^+\right] + F(1 + R_-)K_w/\left[H^+\right]. \tag{38}$$

Substitution of Eq. (38) into Eq. (30) yields our governing differential equation of the system as follows:

$$\frac{1}{r^2}\frac{\partial}{\partial r}\left(r^2 \frac{1}{[H^+]}\frac{\partial [H^+]}{\partial r}\right) = \frac{F}{\varepsilon V_T}\left\{(1 + R_+)[H^+] + (1 + R_-)K_w/[H^+]\right\}. \tag{39}$$

Our boundary conditions of the solution are

$$\nabla\left[H^+\right] = 0 \text{ at center of the droplet}, \tag{40}$$

$$\text{total surface charge} + \iiint_V \rho dV = 0, \tag{41}$$

Published under an exclusive license by AIP Publishing

$$\iiint_V c_+ dV = \text{moles of} + 1 \text{ ion in the droplet}\left(\text{excluding } \mathrm{H}^+\right), \quad (42)$$

and

$$\iiint_V c_- dV = \text{moles of} - 1 \text{ ion in the droplet}\left(\text{excluding } \mathrm{OH}^-\right), \quad (43)$$

where c_+ and c_- are the concentrations of the +1 and −1 valence strong electrolytes, respectively. There are four boundary conditions as it is a second-order differential equation with two unknown parameters (R_+ and R$_-$). The boundary condition given in Eq. (41) ensures that the droplet is net neutral. Adjusting this boundary condition allows for charged droplets to be evaluated. For a charged droplet, the boundary condition given by Eq. (41) is replaced with

$$\text{total surface charge} + \iiint_V \rho dV = \text{net droplet charge}. \quad (44)$$

In the case of a weak acid buffer, Eq. (31) is instead expanded to

$$\rho = F(1 + R_+)\left[\mathrm{H}^+\right] + F(K_w + K_a[HA])/\left[H^+\right]. \quad (45)$$

Substitution of Eq. (45) into Eq. (30) yields our governing differential equation of the weak acid buffered system as follows:

$$\frac{1}{r^2}\frac{\partial}{\partial r}\left(r^2 \frac{1}{[\mathrm{H}^+]}\frac{\partial[\mathrm{H}^+]}{\partial r}\right) = \frac{F}{V_T \varepsilon}\left\{(1 + R_+)[\mathrm{H}^+] + (K_w + K_a[HA])/[H^+]\right\}. \quad (46)$$

There are four boundary conditions as it is a second-order differential equation with two unknown parameters (R_+ and [HA]),

$$\nabla\left[H^+\right] = 0 \text{ at center of the droplet}, \quad (47)$$

$$\text{total surface charge} + \iiint_V \rho dV = \text{net droplet charge}, \quad (48)$$

$$\iiint_V c_+ dV = \text{moles of} + 1 \text{ ion in the droplet}\left(\text{excluding } \mathrm{H}^+\right), \quad (49)$$

and

$$\iiint_V (c_A + c_{HA}) dV = \text{combined moles of acid and conjuagate base in droplet}. \quad (50)$$

The boundary condition in Eq. (50) conserves the sum of A^- and HA species as this is a known quantity in the microdroplet precursor solution and conserved in the transition to a microdroplet.

The above equation and boundary conditions were evaluated using a combination of the MATLAB's® bvp4c differential equation solver and ODE45 equation solver. Calculations were performed assuming a negatively charged surface at 25 °C with a value of ε of water at 25 °C. The calculated distribution of species in the droplet is shown in the results. The MATLAB® code is available on Github (https://github.com/ChristianChamberlayne/Microdroplets-Can-Act-as-Electrochemical-Cells.git).

Pseudo-steady-state condition

A major assumption in this work is that the ion gradients in the droplet remain in pseudo-equilibrium. Essentially, the timescale of the surfactant ion reaction is significantly slower than the timescale for establishing the ion gradients and other chemical equilibria within the droplet. This allows for the microdroplet EDL to be calculated assuming a pseudo-steady-state condition. A series of microdroplets that follow the stoichiometry of main reaction can then be used to calculate the driving force from the microdroplet on the reaction. Once the ion distributions are calculated, the potential energy of the droplets is calculated as described in Eqs. (15)–(20). Looking at the sets of solutions with different surface charges that follow the partial derivatives described in Eqs. (16) and (20) (for ion-to-ion and ion-to-neutral reaction paths, respectively), the change in potential energy per coulomb change in the surface charge gives the effective electrochemical voltage driving that reaction.

ACKNOWLEDGMENTS

The research in this work was supported by the National Institutes of Health under Award No. 1R01EB025867, the Air Force Office of Scientific Research through the Basic Research Initiative (Grant No. AFOSR FA9550-16-1-0113), the Multidisciplinary University Research Initiative (MURI) program (Grant No. AFOSR FA9550-21-1-0170), and a fellowship to CFC from the Center for Molecular Analysis and Design at Stanford University.

REFERENCES

[1]Z. Wei, Y. Li, R. G. Cooks, and X. Yan, "Accelerated reaction kinetics in microdroplets: Overview and recent developments," Annu. Rev. Phys. Chem. **71**, 31–51 (2020).
[2]G. Rovelli, M. I. Jacobs, M. D. Willis, R. J. Rapf, A. M. Prophet, and K. R. Wilson, "A critical analysis of electrospray techniques for the determination of accelerated rates and mechanisms of chemical reactions in droplets," Chem. Sci. **11**(48), 13026–13043 (2020).
[3]N. Narendra, X. Chen, J. Wang, J. Charles, R. G. Cooks, and T. Kubis, "Quantum mechanical modeling of reaction rate acceleration in microdroplets," J. Phys. Chem. A **124**(24), 4984–4989 (2020).
[4]H. Hao, I. Leven, and T. Head-Gordon, "Can electric fields drive chemistry for an aqueous microdroplet?," Nat. Commun. **13**, 280 (2022).
[5]K. R. Wilson, A. M. Prophet, G. Rovelli, M. D. Willis, R. J. Rapf, and M. I. Jacobs, "A kinetic description of how interfaces accelerate reactions in micro-compartments," Chem. Sci. **11**(32), 8533–8545 (2020).
[6]Y. Uematsu, D. J. Bonthuis, and R. R. Netz, "Impurity effects at hydrophobic surfaces," Curr. Opin. Electrochem. **13**, 166–173 (2019).
[7]R. J. Saykally, "Air/water interface: Two sides of the acid-base story," Nat. Chem. **5**(2), 82–84 (2013).
[8]X. Yan, M. Delgado, J. Aubry, O. Gribelin, A. Stocco, F. Boisson-Da Cruz, J. Bernard, and F. Ganachaud, "Central role of bicarbonate anions in charging water/hydrophobic interfaces," J. Phys. Chem. Lett. **9**(1), 96–103 (2018).
[9]C. F. Chamberlayne and R. N. Zare, "Simple model for the electric field and spatial distribution of ions in a microdroplet," J. Chem. Phys. **152**, 184702 (2020).
[10]M. Ahmed, M. Blum, E. J. Crumlin, P. L. Geissler, T. Head-Gordon, D. T. Limmer, K. K. Mandadapu, R. J. Saykally, and K. R. Wilson, "Molecular properties

Published under an exclusive license by AIP Publishing

and chemical transformations near interfaces," J. Phys. Chem. B, **125** 9037–9051 (2021).
[11]S. Ciampi, I. Diez-Perez, M. Coote, and N. Darwish, "Experimentally harnessing electric fields in chemical transformations," in *Effects of Electric Fields on Structure and Reactivity: New Horizons in Chemistry*, edited by S. Shaik and T. Stuyver (Royal Society of Chemistry, 2021).
[12]S. D. Fried and S. G. Boxer, "Electric fields and enzyme catalysis," Annu. Rev. Biochem. **86**, 387–415 (2017).
[13]S. D. Fried, S. Bagchi, and S. G. Boxer, "Extreme electric fields power catalysis in the active site of ketosteroid Isomerase," Science **346**(6216), 1510–1514 (2014).
[14]C. F. Gorin, E. S. Beh, and M. W. Kanan, "An electric field-induced change in the selectivity of a metal oxide-catalyzed epoxide rearrangement," J. Am. Chem. Soc. **134**(1), 186–189 (2012).
[15]K. I. Hilsabeck, J. L. Meiser, M. Sneha, N. Balakrishnan, and R. N. Zare, "Photon catalysis of deuterium iodide photodissociation," Phys. Chem. Chem. Phys. **21**(26), 14195–14204 (2019).
[16]K. I. Hilsabeck, J. L. Meiser, M. Sneha, J. A. Harrison, and R. N. Zare, "Nonresonant photons catalyze photodissociation of phenol," J. Am. Chem. Soc. **141**(2), 1067–1073 (2019).
[17]K. Kang, J. Fuller, A. H. Reath, J. W. Ziller, A. N. Alexandrova, and J. Y. Yang, "Installation of internal electric fields by non-redox active cations in transition metal complexes," Chem. Sci. **10**(43), 10135–10142 (2019).
[18]J. K. Lee, K. L. Walker, H. S. Han, J. Kang, F. B. Prinz, R. M. Waymouth, H. G. Nam, and R. N. Zare, "Spontaneous generation of hydrogen peroxide from aqueous microdroplets," Proc. Natl. Acad. Sci. U. S. A. **116**(39), 19294–19298 (2019).
[19]J. K. Lee, H. S. Han, S. Chaikasetsin, D. P. Marron, R. M. Waymouth, F. B. Prinz, and R. N. Zare, "Condensing water vapor to droplets generates hydrogen peroxide," Proc. Natl. Acad. Sci. U. S. A. **117**(49), 30934–30941 (2020).
[20]J. K. Lee, D. Samanta, H. G. Nam, and R. N. Zare, "Micrometer-sized water droplets induce spontaneous reduction," J. Am. Chem. Soc. **141**(27), 10585–10589 (2019).
[21]D. Gao, F. Jin, J. K. Lee, and R. N. Zare, "Aqueous microdroplets containing only ketones or aldehydes undergo Dakin and Baeyer–Villiger reactions," Chem. Sci. **10**(48), 10974–10978 (2019).
[22]J. K. Lee, D. Samanta, H. G. Nam, and R. N. Zare, "Spontaneous formation of gold nanostructures in aqueous microdroplets," Nat. Commun. **9**(1), 1–9 (2018).
[23]D. I. Hoult, "Solvent peak saturation with single phase and quadrature Fourier transformation," J. Magn. Reson. **21**(2), 337–347 (1976).
[24]C. F. Chamberlayne, R. N. Zare, and J. G. Santiago, "Effects of weak electrolytes on electric double layer ion distributions," J. Phys. Chem. Lett. **11**(19), 8302–8306 (2020).
[25]R. J. Hunter, "Charge and potential distribution at interfaces," in *Zeta Potential in Colloid Science* (Academic Press Limited, London, 1981), pp. 11–58.
[26]A. Malevanets and S. Consta, "Variation of droplet acidity during evaporation," J. Chem. Phys. **138**(18), 184312 (2013).
[27]L. I. Berger, "Dielectric strength of insulating materials," in *CRC Handbook of Chemistry and Physics*, 102nd ed. (CRC Press, Boca Raton, FL, 2021), p. 15–46.
[28]L. I. Berger, "Dissociation constants of organic acids and bases," in *CRC Handbook of Chemistry and Physics*, 102nd ed. (CRC Press, Boca Raton, FL, 2021), p. 5–105.
[29]D. Griffiths, *Introduction to Electrodynamics*, 4th ed. (Pearson Education, Inc., Boston, 1989), p. 94.
[30]C. F. Chamberlayne and R. N. Zare, "What role does the electric double layer play in redox reactions at planar electrostatically charged insulating surfaces?," Top. Catal. (published online 2021).
[31]A. Fallah-Araghi, K. Meguellati, J.-C. Baret, A. E. Harrak, T. Mangeat, M. Karplus, S. Ladame, C. M. Marques, and A. D. Griffiths, "Enhanced chemical synthesis at soft interfaces: A universal reaction-adsorption mechanism in microcompartments," Phys. Rev. Lett. **112**(2), 1–5 (2014).
[32]V. Kwan and S. Consta, "Bridging electrostatic properties between nanoscopic and microscopic highly charged droplets," Chem. Phys. Lett. **746**, 137238 (2020).
[33]D. V. Matyushov, "Electrostatic solvation and mobility in uniform and non-uniform electric fields: From simple ions to proteins," Biomicrofluidics **13**(6), 064106 (2019).
[34]D. Muñoz-Santiburcio and D. Marx, "Confinement-controlled aqueous chemistry within nanometric slit pores," Chem. Rev. **121**(11), 6293–6320 (2021).
[35]R. Probstein *Physicochemical Hydrodynamics*, 2nd ed. (John Wiley & Sons, Inc., New York, 1994), p. 38.
[36]R. Probstein *Physicochemical Hydrodynamics*, 2nd ed. (John Wiley & Sons, Inc., New York, 1994), p. 42.
[37]J. Newman and K. Thomas-Alyea *Electrochemical Systems*, 3rd ed. (John Wiley & Sons, Inc., Hobroken, NJ, 2004), p. 149.

Published under an exclusive license by AIP Publishing